IIETA International Information and Engineering Technology Association
Advancing the World of Information and Engineering

Journal Européen des Systèmes Automatisés
Vol. 55, No. 5, October, 2022, pp. 633-639
Journal homepage: http://iieta.org/journals/jesa

A Barrier Function-Based Variable Structure Control for Maglev System

Taghreed MohammadRidha*, Mina Qays Kadhim

Control and Systems Engineering Department, University of Technology, Baghdad 10066, Iraq

Corresponding Author Email: taghreed.m.ridha@uotechnology.edu.iq

https://doi.org/10.18280/jesa.550508

Received: 13 June 2022
Accepted: 6 October 2022

Keywords:
magnetic levitation, variable structure control, adaptive control, sliding mode control, invariant set, barrier function

ABSTRACT

Magnetic levitation (Maglev) systems are widely employed in the industry especially in mechatronics systems for precise positioning and suspension. They are inherently unstable having nonlinear models with uncertain parameters and exposed to external disturbances. Therefore, high-performance robust control designs are recommended for these systems. An Adaptive Variable Structure Controller based on barrier function (AVSCbf) is designed for the first time in this work to control the displacement of the ball position of a disturbed Maglev system. This approach does not require prior knowledge of the disturbance upper bounds in the design procedure. The state space region defined by the barrier function is designed to be attractive and invariant. This feature is essential to reject disturbances and handle parametric uncertainties. The adaptive law is activated when the state trajectory is initiated outside the invariant set defined by the barrier function. The gain of the VSC is adapted according to an adaptation law, which considers the system input constraints. The control input is constrained to be a bounded positive quantity. The adaptive VSC is only applied during the reaching phase. Once the state reaches the invariant set, the barrier-function-based VSC is applied to confine the state inside it. The resulting overall controller is a chattering-free VSC since the barrier-function based VSC is continuous. The steady-state error is limited to a minimal value by only specifying the barrier function parameter. Numerical simulations are conducted to show the efficiency of the new approach. Three types of VSC controllers for the Maglev system are compared. AVSCbf is compared to the performance of adaptive only VSC without the barrier function (AVSC) and both are designed in this work. AVSCbf is also compared to the classical VSC performance from previous work in the literature. The results of the comparison showed the efficiency of the proposed controller.

1. INTRODUCTION

The Magnetic levitation (Maglev) system is a well-known solution for motion control systems such as in Maglev trains and in the high-precision manufacturing facilities. They are frictionless electromechanical devices providing energy losses elimination that is widely employed in the industry such as magnetic levitation trains, wind tunnels and high-precision positioning platforms. However, controlling these systems is challenging due to their off-control instability and inherent nonlinearity. Moreover, Maglev system models have parameter uncertainty and maybe exposed to external disturbances.

Many control algorithms have been designed in the literature for this system. A comparative study was conducted in Yaseen and Abd [1] by designing Linear Quadratic Regulator (LQR), a PID controller and a lead compensator. The results showed that LQR provided higher stability and better performance. Among effective, robust control approaches that are successfully employed in this system's literature is the Variable Structure Control theory (VSC) and especially Sliding Mode Control (SMC). Zhang et al. [2] used the exact feedback linearization method to realize exact linearization and decoupling, and SMC based on disturbance observer is designed to compensate for uncertainties and disturbances. Numerical and experimental results showed the effectiveness of the controller with and without an observer. A nonlinear disturbance observer and an extended state observer for a nonlinear active magnetic bearing system are designed by Giap and Huang [3] to compensate for disturbance and parameter uncertainty, respectively. A fuzzy SMC was designed based on the estimation results of the observers. Fuzzy logic was used to find the boundary layer of the sliding mode controller.

Adaptive SMC (ASMC) is designed and applied by Al-Samarraie et al. [4] for an uncertain Maglev model to stabilize a steel ball at the desired position. A sliding mode differentiator was employed to estimate the ball velocity. The robust controller effectiveness was verified experimentally. On the other hand, adaptive terminal SMC based on the disturbance compensation technique is proposed by Wang et al. [5]. The discontinuous gain is adapted to avoid high gain and thus reduce chattering. Fuzzy-PI adaptive sliding control (Fuzzy-ASMC) is designed by Mourad and Youcef [6] for the Maglev system. Fuzzy-PI is designed to replace the discontinuous term to alleviate the chattering of SMC. Al-Samarraie [7] designed a positive continuous VSC with a predetermined steady-state error to sustain the steel ball of a Maglev in the presence of an external disturbance and parameter uncertainty. The control signal is the squared value of the electric current, which is considered in the design as a positive input constraint. The attraction area was also

determined for the control system, and the numerical results confirmed the system's robustness in different simulation scenarios. Adaptive robust nonlinear SMC for the vertical position of the Maglev system is proposed by Alain [8]. The bound of uncertainty was assumed to be known.

Most previous studies either estimated the perturbation or used the knowledge of its upper bounds in the design. Recently, a new VSC design strategy has been proposed by Obeid et al. [9] for a class of disturbed systems without the need for the upper bounds of the perturbations/uncertainties. The significant advantage of this approach is that there is no overestimation of the control gain; therefore, chattering is prevented. The chattering problem in VSC was solved in the literature by replacing the discontinuous term of the control law by adding a smoothing approximation, like adding a boundary layer. Muntashir et al. [10] for instance. Moreover, the steady-state error can be bounded by only selecting the barrier function parameter. This approach was successfully employed in several applications [11-17].

In this work, a positive adaptive-barrier-strategy-based VSC is designed for the first time to control the displacement of a disturbed Maglev system. The system model is nonlinear, unstable, uncertain and exposed to unknown disturbances. Its performance is compared to two other controllers to show the efficiency of the new robust adaptive control strategy. AVSCbf is compared to adaptive only VSC (AVSC) without the barrier function. It is also compared to the performance of the classical VSC designed earlier in Al-Samarraie [7]. The latter's design procedure was based on the knowledge of the upper bounds of the perturbations. AVSCbf has the following main features over the other robust controllers:

(1) It does not require the upper bounds of the unknown perturbation (disturbance/uncertainties) in the design, reducing the design complexity.

(2) Only the barrier function parameter is to be selected which identifies the invariant neighborhood of the switching manifold. The smaller this parameter is, the smaller the steady-state error of the controlled variable.

(3) The proposed VSC is continuous, and chattering is prevented since the barrier function is differentiable.

(4) The gain of this strategy is not overestimated and is used to steer the trajectory to a predefined neighborhood of zero.

This paper is organized as follows: The next section describes the Maglev system dynamics and state variables. Section 3 provides some necessary definitions. Section 4 presents the design of the adaptive VSC. AVSCbf is designed in Section 5. The simulation results in two different scenarios are illustrated in Section 6 that compares VSC, AVSC and AVSCbf. Finally, Section 7 presents the conclusion of this work.

2. MATHEMATICAL MODEL OF MAGNETIC LEVITATION

The Maglev system consists of a magnetic suspension system whose objective is to vertically control the steel ball position by controlling the electromagnet current as illustrated in Figure 1. The coil current and the position of the steel ball are the main variables that describe the system model equations as follows:

$$\ddot{x} = g - \phi(x)i^2 + d(t) \tag{1}$$

where,

$$\phi(x) = \frac{Q}{2M(X_\infty + x)^2} \tag{2}$$

where, $x[m]$ is the ball position, $g[m/s^2]$ is the gravity acceleration, $i(t)$[A] is the coil current and $M[kg]$ is the steel ball mass. Q and X_∞ are positive constants determined by the the coil, magnetic core and steel ball characteristics. $d(t)$[m/s^2]represents the unknown external disturbance. Notice that the attractive force of the ball is proportional to the square of the electric current $F_{em}=\phi(x)i^2$ i.e., the system has a unidirectional control input $u=i^2$.

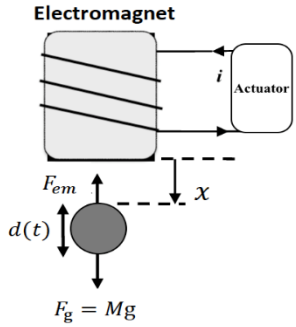

Figure 1. Schematic diagram of maglev system

Maglev system model in Eq. (1) will be represented in terms of the error variable (e_1=x-x_d) in state space as follows:

$$\dot{e}_1 = e_2 \tag{3}$$

$$\dot{e}_2 = g - \phi(x)u + d(t) - \ddot{x}_d \tag{4}$$

3. PRELIMINARIES

Definition 1 [9]: Given a constant ϵ>0, a barrier function is defined as an even continuous function $f: z \in]-\epsilon, \epsilon[\rightarrow g(z) \in [b, \infty[$ strictly increasing on [0, ϵ].

- $lim_{|z|\rightarrow\epsilon} g(z) = \infty_+$
- $g(z)$ has a unique minimum at zero and $g(0)=b\geq 0$.

Here, there are two different classes of BFs:

(1) Positive-definite BF (PBF): $g_p(z) = \frac{\epsilon F}{\epsilon - |z|}, g_p(0) = F.$

(2) Positive Semi-definite BF (PSBF): $g_{ps}(z) = \frac{|z|}{\epsilon - |z|}, g_{ps}(0) = 0.$

Definition 2 The notation $[]_+$ is used to represent the following positive Function:

$$[F]_+ = \begin{cases} 1 & F > 0 \\ 0 & F \geq 0 \end{cases} \tag{5}$$

4. ADAPTIVE VSC DESIGN

The preferred robustness of VSC is faced with two problems: the high-amplitude chattering of the discontinuous control and the large gain of the control action. One solution to these problems is to employ an adaptation law to maintain the VSC gain at a minimum sufficient value. The idea is to reduce or even eliminate chattering and produce minimum control effort

to preserve the sliding manifold's global or semi-global attractiveness.

In this section, an adaptive positive VSC is designed so that the discontinuous gain is adapted according to the current control constraints of the Maglev system. Adaptive sliding mode controllers have been developed in Ref. [18] based on two different algorithms for bounded uncertainties and perturbations that are unknown. The first adaptive law evaluates the unknown uncertainties/perturbation using the concept of equivalent control that employs a low-pass filter. The second adaptive algorithm does not estimate the bounds of perturbations/uncertainties and establishes a real sliding mode. In this work, the second approach is used as it requires a smaller amount of tuning parameters [19].

The sliding manifold for the system Eq. (3) and (4) is designed as follows:

$$s = e_2 + \lambda e_1 \tag{6}$$

where, λ is a positive parameter defining the slope of s, according to sliding mode control theory, whenever the sliding manifold is reached s=0, asymptotic stability for the error dynamics is established in (7): $e \rightarrow 0$ as $t \rightarrow \infty$.

The adaptive VSC law $u=u_a$ is designed as follows considering the maximum allowable control for the Maglev system u_{max}:

$$u = \begin{cases} u_a & u \le u_{max} \\ u_{max} & u > u_{max} \end{cases} \tag{7a}$$

$$u_a = \frac{K(t)}{\phi_o(x)}[sign(s)]_+ \tag{7b}$$

where, $\phi_o(x)$ is the nominal value of $\phi(x)$ in Eq. (4). $K(t)$ is the adaptive discontinuous gain is designed as follows [20]:

$$K(t) = \begin{cases} \mu(t) & 0 < \mu(t) < u_{max} \\ u_{max} & \mu(t) \ge u_{max} \\ 0.25u_{max} & \mu(t) < 0 \end{cases} \tag{8}$$

$$\dot{\mu}(t) = \rho|s|[sign(s)]_+ sign(|s| - \epsilon) \tag{9}$$

where, ρ, ϵ>0. The adaptive gain, in this case, does not require the disturbance bound that was used earlier to design the controller in ref. [7]. Thus, it overcomes the design complexity and the prior knowledge of the disturbance/uncertainties bounds.

Define $\delta(t, x)$ as a function that contains all the unknown perturbations including the disturbance $d(t)$ and any parametric uncertainties in (4):

$$\delta(t,x) = g - \Delta\phi(x)u + d(t) - \ddot{x}_d + \lambda e_2 \tag{10}$$

where, $\Delta\phi(x)=\phi(x)-\phi_o(x)$ is uncertainty in $\phi(x)$. The perturbation function $\delta(t, x)$ is assumed unknown but bounded as follows:

$$|\delta| \le \delta_{max} \tag{11}$$

where, δ_{max} is the unknown positive bound. Considering the dynamics of the sliding manifold by differentiating Eq. (6):

$$\dot{s} = -u + \delta(t,x) \tag{12}$$

The adaptive law in (7) and (8) is used to steer s to reach the neighborhood of switching manifold $\Omega=\{x:|s|\le\epsilon\}$ in finite time [6, 13, 15]. The adaptive gain of AVSC increases until reaching the set Ω then it decreases gradually to some value that permits compensating for the disturbance. However, as shown in simulation results, when the disturbance grows, the state leaves Ω [6, 15]. The gain increases to compensate for the disturbance to reach the surface again. In other words, Ω is not invariant with AVSC since the state can leave it many times whenever a sudden disturbance change occurs, which is the main drawback of AVSC that degrades its performance since the steady-state error cannot be bounded to a predefined value. For this reason, AVSCbf is designed next. The adaptive law in (7) and (8) is used to steer the s to reach Ω in finite time [9]. Then, the adaptive law switches to the BF that can confine s in the predefined set Ω. This set is invariant as given by the barrier function defined earlier. The steady- state error, in this case, is small and bounded and depends on the choice of ϵ that defines the size of Ω.

5. ADAPTIVE BARRIER-FUNCTION-BASED VSC DESIGN

The PSBF is used in this work. AVSCbf is designed as follows so that the barrier function-based VSC is activated whenever the barrier region is reached i.e.

$$u = \begin{cases} \begin{cases} u_a & |s| > 0.5\epsilon \\ \lambda_f \frac{|s|}{\epsilon - |s|} \frac{[sign(s)]_+}{\phi_o(x)} & |s| \le 0.5\epsilon \end{cases} & u \le u_{max} \\ u_{max} & u > u_{max} \end{cases} \tag{13}$$

where, λ_f>1 is a gain to further reduce the steady-state error inside the invariant set as will be shown later. The AVSC (u_a) in Eq. (13) is active once only to drive the state trajectory to the positively invariant set Ω which is done in some finite time t_{bf} [8]. Once the trajectory enters Ω, then AVSCbf is on to maintain it inside, i.e. $x(t) \in \Omega \forall t \ge t_{bf}$.

Remark 1: The discontinuous gain in classical VSC requires the knowledge of the bounds of the perturbation/uncertainties, while in the proposed approach the bounds are not needed. The only variable to be selected is a suitable value for ϵ to achieve the desired accuracy.

Remark 2: The proposed VSC in Eq. (13) is continuous in Ω. The chattering will be eliminated (or at least attenuated for small ϵ). Moreover, the steady-state error as a function of ϵ and is smaller for smaller ϵ.

Remark 3: Choosing the parameter λ_f>1 is helpful in further attenuating the perturbations and strengthening the attractiveness of the set Ω by showing $s\dot{s}$<0 as follows; using Eq. (12):

$$s\dot{s} = s(-u + \delta(t,x)) \tag{14}$$

Inside Ω, the BF control law of Eq. (13) is active in this case. Thus, employing it in Eq. (14).and taking the upper bounds yields:

$$s\dot{s} \le |s|(|\delta(t,x)| - \lambda_f \frac{|s|_+}{|\epsilon - |s||}) \tag{15}$$

where, s is near ϵ, $\lambda_f \frac{|s|_+}{|\epsilon-|s||} > |\delta(t,x)|$, thus ss<0 and the set Ω is attractive and the state remain in it.

In the next section, AVSCbf will be compared to AVSC in Eq. (7) and Eq. (8). The latter is discontinuous and suffers from chattering. The undesired chattering of AVSC will be eliminated or attenuated to have a good comparison, which is achieved by replacing the sign function in its control law with the following Function [7]:

$$q(s) = \begin{cases} \frac{s}{\eta} & 0 < s \leq \eta \\ [sign(s)]_+ & otherwise \end{cases} \quad (16)$$

so, that Eq. (7b) becomes

$$u_a = \frac{K(t)}{\phi_o(x)} q(s) \quad (17)$$

where, η>0 is a design parameter that defines the boundary layer around the surface s for this controller. The chattering will be reduced by using Function (16).

6. SIMULATION RESULTS AND DISCUSSION

The performance of the proposed approach is tested by numerical simulations using the Scilab simulation platform. The nominal parameters of the Maglev system are as given in [5, 12] and presented in Table 1. The controllers' parameters are in Table 2. The VSC designed earlier in [7] will be applied here to compare it to AVSC and AVSCbf performances designed for the first time in this work. The classical VSC is designed in a detailed procedure depending on the disturbance's upper bound and Maglev system parameters uncertainties. The final VSC control law is as follows [7]:

$$u = \begin{cases} \frac{H[H]_+[sign(s)]_+}{\phi_o(x)(1-\alpha)} & u \leq u_{max} \\ u_{max} & u > u_{max} \end{cases} \quad (18)$$

where, $H = g_o - \ddot{x}_d + \lambda e_2 + d^+ + k_o$, $\delta_{max} = \alpha\phi_o(x)u + d^+$and $k_o, \alpha, d^+ > 0$.

As derived in [7], VSC gain H is obtained through a detailed, precise design procedure considering the perturbation's upper bounds. Moreover, this classical VSC is discontinuous and hence causes the undesired chattering phenomenon. Therefore, the designer had to approximate the discontinuous sign function using the saturation function in Eq. (16) to avoid chattering. Even though the sliding manifold, in this case, is no more attractive, it can be shown that the steady-state error will be limited positively invariant $\Omega_c = \{x: 0 < (x - x_d) < \frac{\eta}{\lambda}\}$.

The simulations are conducted in two scenarios where the results of three controllers VSC, AVSC and AVSCbf, are compared.

6.1 Scenario I

The desired ball position is fixed here at x_d=0.01m, $\dot{x}_d = 0m/s$. The system is exposed to an unknown external acceleration $d(t)$=2sin(4πt)m/s^2. The initial condition is taken as $x(0) = 0.008m, \dot{x}(0) = 0.01m/s$ which is considered one of the worst-case scenarios because $s(0)$<0 and thus all three controllers are temporarily off. The state trajectory is initiated below the sliding manifold, i.e. $s(0)$<0 as shown in Figures 2 and 3. This scenario is designed so that the ball is initiated vertically above the desired position and depends on the gravity force first to hit x_d=0.01 which means that the three controllers are temporarily off, as shown in Figures 4 and 5. Despite that, the surface is attractive for each controller in this region.

Table 1. Maglev system parameters

Parameter	$Q[H.m]$	$M[kg]$	$X_\infty[m]$	g[m/s^2]
Nominal Values	0.00145	0.5	0.0085	9.81
Real (Unknown) Values	0.00165	0.55	0.008	9.81

Table 2. Control parameters

Parameter	Value
u_{max}	25
λ	25
ϵ	0.002
η	0.001
$\mu(0)$	u_{max}
ρ	8000
λ_f	40

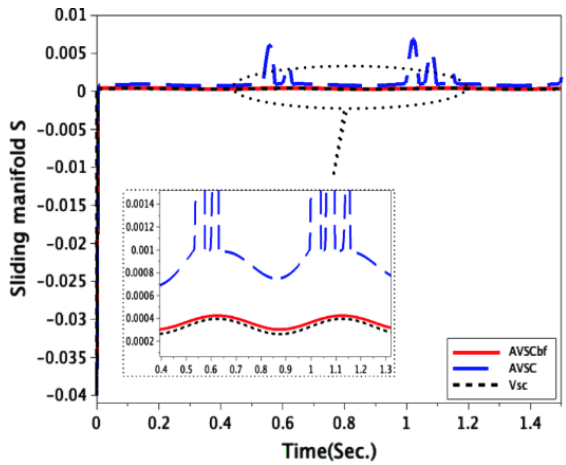

Figure 2. Switching surface $s(t)$ of Scenario I: dotted line for VSC, dashed line for AVSC and solid line for AVSCbf

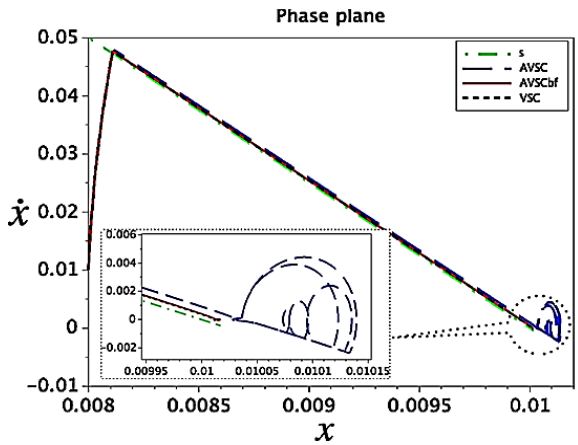

Figure 3. State trajectory in phase plane of Scenario I: dotted line for VSC, dashed line for AVSC and solid line for AVSCbf

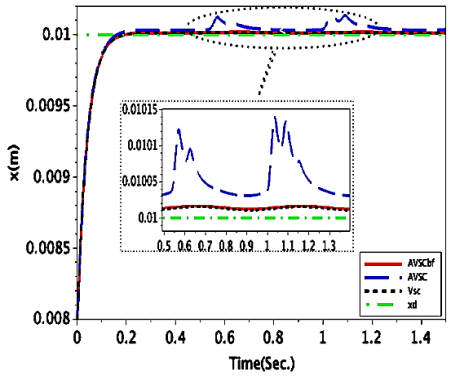

Figure 4. Ball position of Scenario I: dotted line for VSC, dashed line for AVSC and solid line for AVSCbf. Dash-dot line for desired position

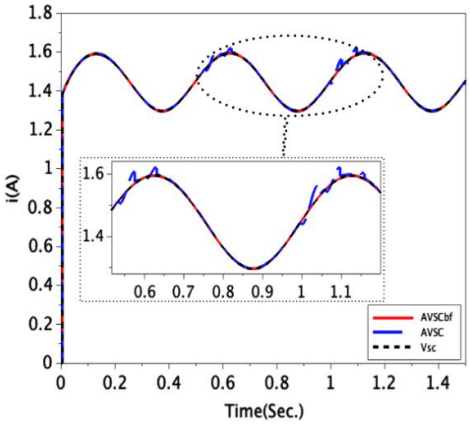

Figure 5. Control current i(t) of Scenario I: dotted line for VSC, dashed line for AVSC and solid line for AVSCbf

In this scenario, the steady-state error of the ball displacement using AVSCbf was less than that of AVSC, and a better disturbance rejection is yielded, as shown in Figure 4. The disturbance influences AVSC performance, and the trajectory leaves Ω as it is not an invariant set for AVSC case as explained earlier. Thus, the steady-state error increases accordingly. On the other hand, AVSCbf and VSC maintain robust behavior, as illustrated in Figures 2, 3 and 4. For AVSCbf, the state remains inside the invariant set Ω, while VSC maintains it inside the invariant set Ω_c. The size of each invariant set depends mainly on the choice of their parameters: ϵ and η/λ respectively. AVSCbf and VSC performances are similar, bearing in mind that the latter was carefully designed, taking the perturbation bound into account. Moreover, AVSCbf does not produce chattering in the invariant neighborhood of s. Thus, no low pass filtering nor continuous approximation is needed.

6.2 Scenario II

In this case study, the desired ball position is variable x_d=0.01+0.007sin(2πt). The unknown disturbance considered in this case has a sudden amplitude change as follows: $d(t) = 2sin(4\pi t)$ for 0≤t<0.5T_f and $d(t)$=12+2sin(4πt) for 0.5 T_f≤t≤T_f, T_f=1.5sec. is the simulation time. The initial condition is taken as in scenario I. The VSC and AVSC controlled systems behaviors compared to AVSCbf are shown in Figure 6. The ball tracks the desired path until the sudden increase of the disturbance where the ball drifts away temporarily under AVSC at t≥0.5T_f while the VSC and AVSCbf responses are not influenced, and the disturbance is totally rejected. Notice that the velocity of the ball suddenly ripples aggressively during the disturbance change with AVSC, as illustrated in Figure 7. This effect appears in the switching function $s(t)$ where in the case of AVSCbf and classical VSC, it does not leave the predefined neighborhood around zero of Ω and Ω_c respectively. Conversely, as shown in Figure 8, the size of the neighborhood of zero into which $s(t)$ converges by AVSC changes following the disturbance amplitude. The current control action $i = \sqrt{u}$ of each controller is presented in Figure 9.

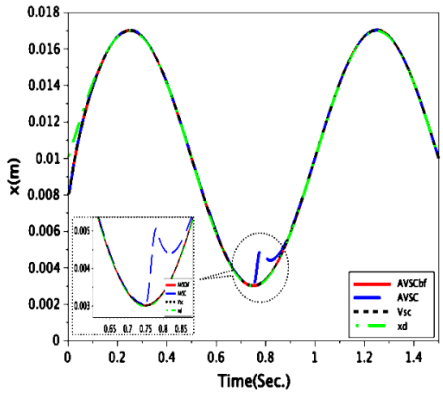

Figure 6. Ball position of scenario II: dotted line for VSC, dashed line for AVSC and solid line for AVSCbf. Dash-dot line for desired position

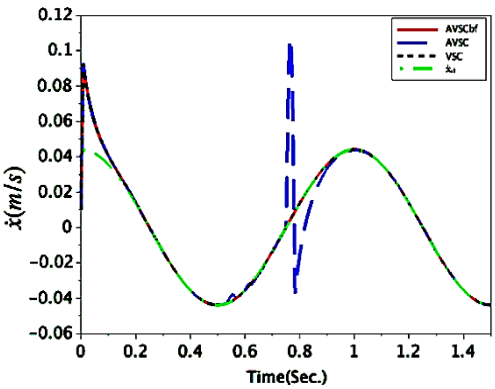

Figure 7. Ball velocity of Scenario II: dotted line for VSC, dashed line for AVSC and solid line for AVSCbf. Dash-dot line for desired velocity

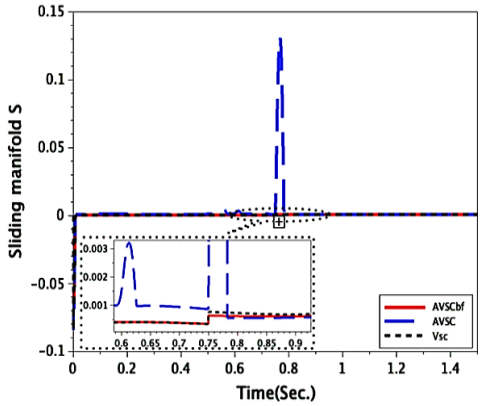

Figure 8. Sliding surface s(t) of Scenario II: dotted line for VSC, dashed line for AVSC and solid line for AVSCbf

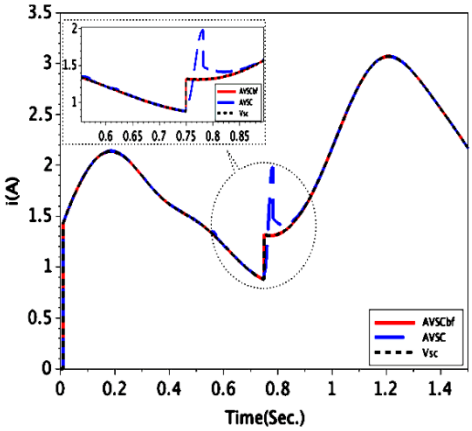

Figure 9. Control current i(t) of Scenario II: dotted line for VSC, dashed line for AVSC and solid line for AVSCbf

7. CONCLUSIONS

This paper proposes a barrier strategy for adapting the gain of the VSC law to control the position of a Maglev disturbed system for the first time. The barrier strategy (AVSCbf) performance is compared to adaptive VSC without the barrier strategy (AVSC) designed in this work. AVSCbf and AVSC control systems are compared to the classical VSC designed in previous work from the literature. Two different simulation scenarios were taken where the desired ball position is fixed and varied. The unknown disturbance in the second scenario changed the amplitude unexpectedly. The upper bound of the disturbance is unknown and not required throughout the design procedure of AVSCbf. The adaptive gain in AVSCbf approach is not overestimated and is used to reach the barrier function invariant set. AVSCbf guaranteed the convergence of the switching variable and confined it inside the predefined neighborhood of zero. As a result, the ball robustly followed the desired reference and was not affected by the perturbation. On the other hand, this neighbourhood was violated using AVSC in response to the disturbance amplitude, which temporarily let the ball leave the desired reference. It is shown that classical VSC performance is comparable to that of AVSCbf with the preferred features of the latter. Both keep the state inside their own invariant sets. However, VSC is designed carefully depending on the knowledge of perturbation bounds, unlike AVSCbf, which does not require this information. AVSCbf provides accuracy for the output variable by choosing one design parameter. Moreover, the latter is continuous, a feature not found in AVSC and VSC. The proposed control algorithm could be compared to Integral SMC based on barrier function as future work. Practical implementation of the controlled system is also proposed to confirm the simulation results.

REFERENCES

[1] Yaseen, M.H., Abd, H.J. (2018). Modeling and control for a magnetic levitation system based on SIMLAB platform in real time. Results in Physics, 8: 153-159. https://doi.org/10.1016/j.rinp.2017.11.026

[2] Zhang, S., Ma, S., Wang, W. (2018). Sliding mode control based on disturbance observer for magnetic levitation positioning stage. Journal of Electrical Engineering and Technology, 13(5): 2116-2124. https://doi.org/10.5370/JEET.2018.13.5.2116

[3] Giap, V.N., Huang, S.C. (2020). Effectiveness of fuzzy sliding mode control boundary layer based on uncertainty and disturbance compensator on suspension active magnetic bearing system. Measurement and Control, 53(5-6): 934-942. https://doi.org/10.1177/0020294020905044

[4] Al-Samarraie, S.A., Midhat, B.F., Al-Deen, R.A.B. (2018). Adaptive sliding mode control for magnetic levitation system. Al-Nahrain Journal for Engineering Sciences, 21(2): 266-274. https://iasj.net/iasj/pdf/daae95ee5d682c90

[5] Wang, J., Zhao, L., Yu, L. (2020). Adaptive terminal sliding mode control for magnetic levitation systems with enhanced disturbance compensation. IEEE Transactions on Industrial Electronics, 68(1): 756-766. https://doi.org/10.1109/TIE.2020.2975487

[6] Mourad, A., Youcef, Z. (2022). Adaptive sliding mode control improved by fuzzy-PI controller: Applied to magnetic levitation system. Engineering Proceedings, 14(1): 14. https://doi.org/10.3390/engproc2022014014

[7] Al-Samarraie, S.A. (2018). Variable structure control design for a magnetic levitation system. Journal of Engineering, 24(12): 84-103. https://doi.org/10.31026/j.eng.2018.12.08

[8] Alain, K.S.T., Fabien, K., Martin, S.S., Bertrand, F.H. (2021). Robust nonsingular sliding mode control of the maglev train system: Case study. SN Applied Sciences, 3(3): 1-18. https://doi.org/10.1007/s42452-021-04341-w

[9] Obeid, H., Fridman, L. M., Laghrouche, S., Harmouche, M. (2018). Barrier function-based adaptive sliding mode control. Automatica, 93: 540-544. https://doi.org/10.1016/j.automatica.2018.03.078

[10] Muntashir, A.A., Purwanto, E., Sumantri, B. (2022). Chattering reduction using boundary-SMC on low-speed setting of 3-phase induction motor with IFOC method. International Review of Automatic Control, 15(1): 1-11. https://doi.org/10.15866/ireaco.v15i1.21250

[11] Ayyarao, T.S. (2019). Modified vector controlled DFIG wind energy system based on barrier function adaptive sliding mode control. Protection and Control of Modern Power Systems, 4(1): 1-8. https://doi.org/10.1186/s41601-019-0119-3

[12] Abd, A.F., Al-Samarraie, S. (2021). Integral sliding mode control based on barrier function for servo actuator with friction. Engineering and Technology Journal, 39(2): 248-259. http://dx.doi.org/10.30684/etj.v39i2A.1826

[13] Liu, Z., Pan, H. (2020). Barrier function-based adaptive sliding mode control for application to vehicle suspensions. IEEE Transactions on Transportation Electrification, 7(3): 2023-2033. https://doi.org/10.1109/TTE.2020.3043581

[14] Zhang, Y., Xian, B., Ma, S. (2015). Continuous robust tracking control for magnetic levitation system with unidirectional input constraint. IEEE Transactions on industrial Electronics, 62(9): 5971-5980. https://doi.org/10.1109/TIE.2015.2434791

[15] Husain, S.S., MohammadRidha, T. (2022). Integral sliding mode controlled ATMD for buildings under siesmic effect. International Journal of Safety and Security Engineering, 12(4): 413-420. https://doi.org/10.18280/ijsse.120401

[16] Husain, S.S., MohammadRidha, T. (2022). Integral

sliding mode control for siesmic effect regulation on buildings using ATMD and MRD. Journale Européen des Systèmes Automatisés, 55(4): 541-548. https://doi.org/10.18280/jesa.550414

[17] Husain, S.S., MohammadRidha, T. (2022). Design of integral sliding mode control for siesmic effect regulation on buildings with unmatched disturbance. Mathematical Modelling of Engineering Problems, 9(4): 1123-1130. https://doi.org/10.18280/mmep.090431

[18] Plestan, F., Shtessel, Y., Bregeault, V., Poznyak, A. (2010). New methodologies for adaptive sliding mode control. International Journal of Control, 83(9): 1907-1919. https://doi.org/10.1080/00207179.2010.501385

[19] Abed, A.F. (2021). Sliding mode controller for motor-quick return servo mechanism. M. Sc. Thesis submitted to Control and Systems Eng. Dept., University of Technology-Iraq, 2021. https://www.researchgate.net/publication/335125969_Sliding_Mode_Control_for_Position_Tracking_of_Servo_System_with_a_Variable_Loaded_DC_Motor.

[20] Al-samarraie, S.A., Ali, L.F. (2018). Output feedback adaptive sliding mode control design for a plate heat exchanger. Al-Nahrain Journal for Engineering Sciences, 21(4): 549-555. https://doi.org/10.29194/NJES.21040549